**Supporting Information:**

# Tetrahedral Structure and Luminescence Properties of Bi-Metallic $Pt_1Ag_{28}(SR)_{18}(PPh_3)_4$ Nanocluster

Xi Kang,[a] Meng Zhou,[b] Shuxin Wang,[a] Shan Jin,[a] Guodong Sun,[a] Manzhou Zhu[a,*] & Rongchao Jin[b,*]

[a]Department of Chemistry and Center for Atomic Engineering of Advanced Materials, Anhui University, Hefei, Anhui 230601, China.
[b]Department of Chemistry, Carnegie Mellon University, Pittsburgh, Pennsylvania 15213, United States.

**Structural analyses of $Pt_1Ag_{28}$, $Au_1Ag_{28}$ and $Ag_{29}$**

Structurally, the previous studies suggested that the structure and composition of the metal core significantly affect the M-S bond lengths. Thus the bond lengths and angles in $Pt_1Ag_{28}$ were compared with the related ones in $Ag_{29}$ and $Au_1Ag_{28}$ (Table S2). Compared the bond lengths in $Pt_1Ag_{28}$ with $Ag_{29}$ and $Au_1Ag_{28}$, the range is larger ($Au_1Ag_{28}$ is similar with $Ag_{29}$ owing to the almost identified framework) although the average bond length is very similar. Regarding to the angles of P-Ag-S on the same motifs, the average angles of $Ag_{29}$ and $Pt_1Ag_{28}$ is 106.91° and 105.94°, respectively. However the average angles in $Pt_1Ag_{28}$ is 126.80, which varies substantially with $Ag_{29}$ ($Au_1Ag_{28}$).

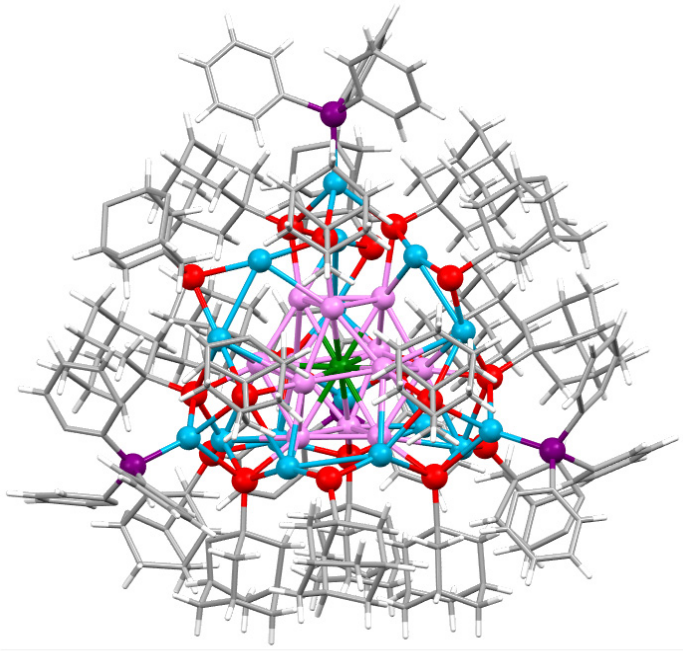

**Fig. S1.** The total structure of $Pt_1Ag_{28}(S\text{-}Adm)_{18}(PPh_3)_4$. Color legend: green sphere, Pt; cerulean sphere, Ag on the shell; violet sphere, Ag in the kernel; red sphere, S; purple sphere, P. For clarity, C and H are shown in wireframe.

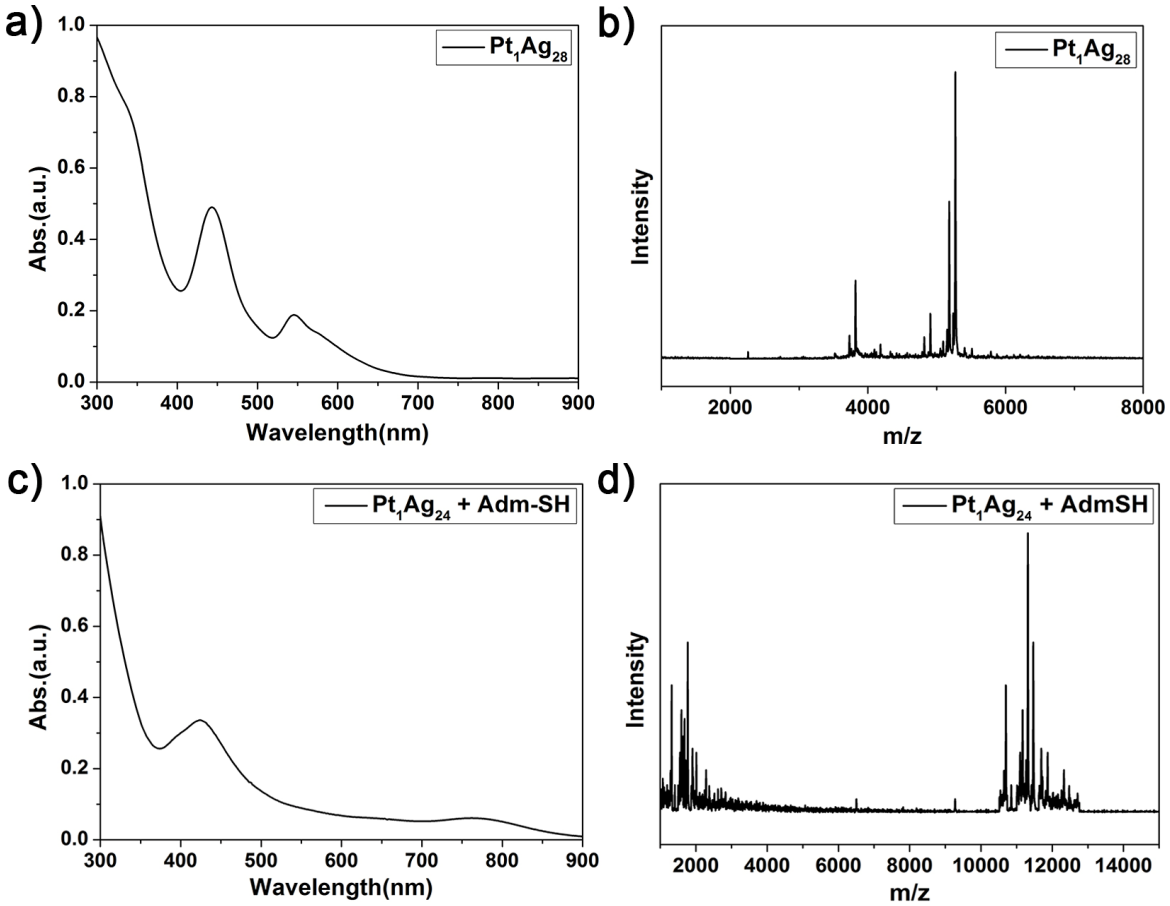


**Fig. S2.** a) UV-Vis spectrum of $Pt_1Ag_{28}$; b) MALDI-MS spectrum of $Pt_1Ag_{28}$; c) UV-Vis spectrum of $Pt_1Ag_{24}$ etching by Adm-SH only ; d) MALDI-MS spectrum of $Pt_1Ag_{24}$ etching by Adm-SH only.

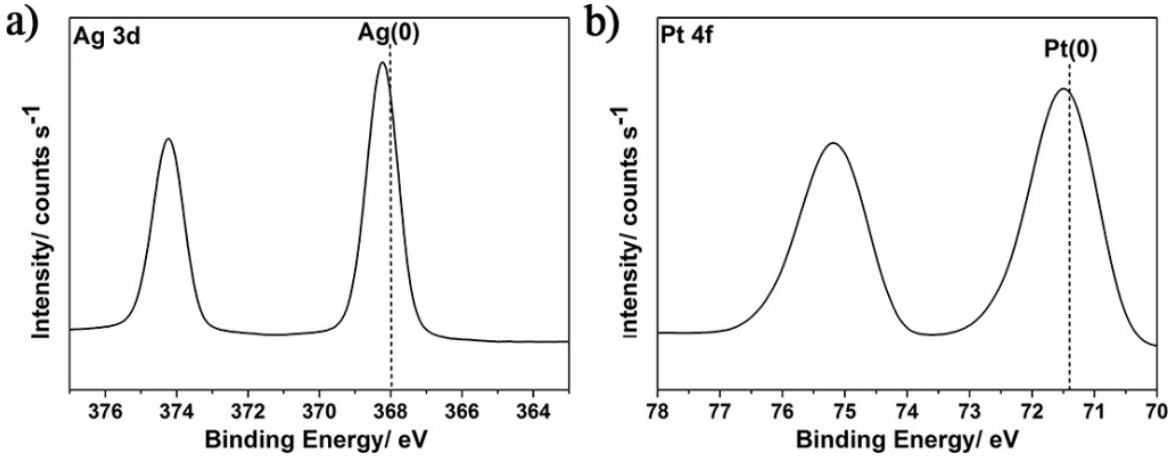


**Fig. S3.** X-ray photoelectron spectroscopy (XPS) of a) Ag 3d, b) Pt 4f in $Pt_1Ag_{28}(S\text{-}Adm)_{18}(PPh_3)_4$ nanocluster.

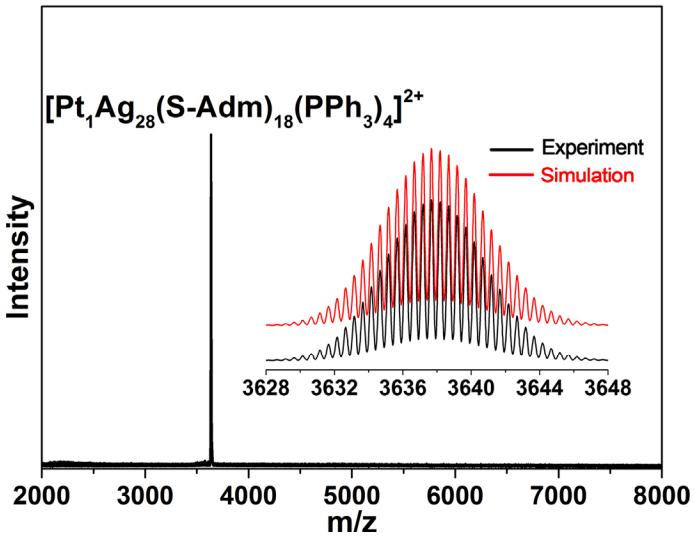


**Fig. S4.** ESI-MS mass spectrum of $Pt_1Ag_{28}$ in positive-mode. Insets: the experimental (black) and simulated (red) isotope patterns of $Pt_1Ag_{28}$.

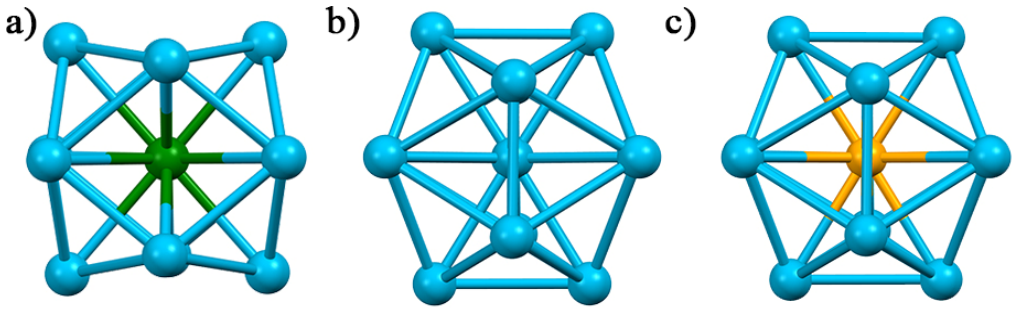


**Fig. S5.** The $M_{13}$ kernel of a) $Pt_1Ag_{28}$, b) $Ag_{29}$ and c) $Au_1Ag_{28}$ nanoclusters. Color legend: green sphere, Pt; cerulean sphere, Ag.

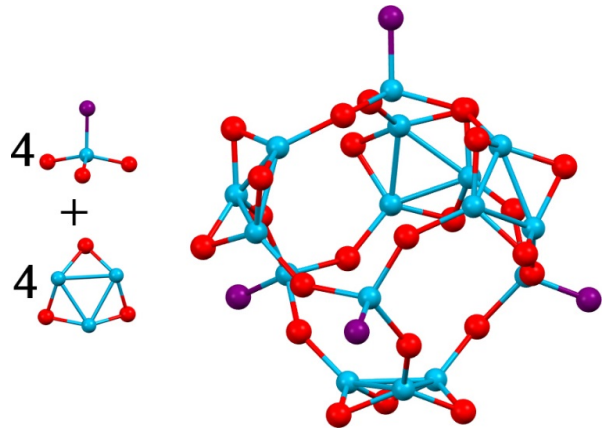


**Fig. S6.** The motifs in $Ag_{29}$ and $Au_1Ag_{28}$ nanoclusters. The overall motif could be separated into 4 $Ag_1S_3P_1$ and 4 $Ag_3S_3$ motifs. Color legend: cerulean sphere, Ag; red sphere, S; purple sphere, P.

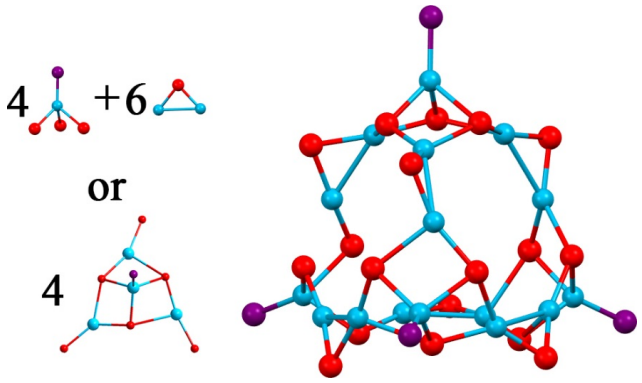


**Fig. S7.** The motifs in $Pt_1Ag_{28}$ nanocluster. The overall motif could be separated into 4 $Ag_1S_3P_1$ and 6 $Ag_2S_1$ motifs or 4 $Ag_4S_6P_1$ motifs sharing 6 S atoms. Color legend: cerulean sphere, Ag; red sphere, S; purple sphere, P.

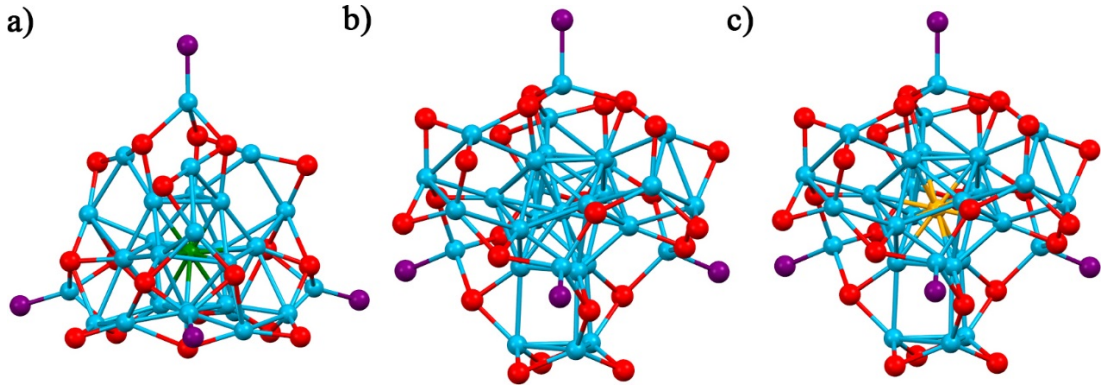


**Fig. S8.** Total structure of a) $Pt_1Ag_{28}$, b) $Ag_{29}$ and c) $Au_1Ag_{28}$ nanoclusters. Color legend: green sphere, Pt; cerulean sphere, Ag; orange sohere, Au; red sphere, S; purple sphere, P. For clarity, C and H are not shown.

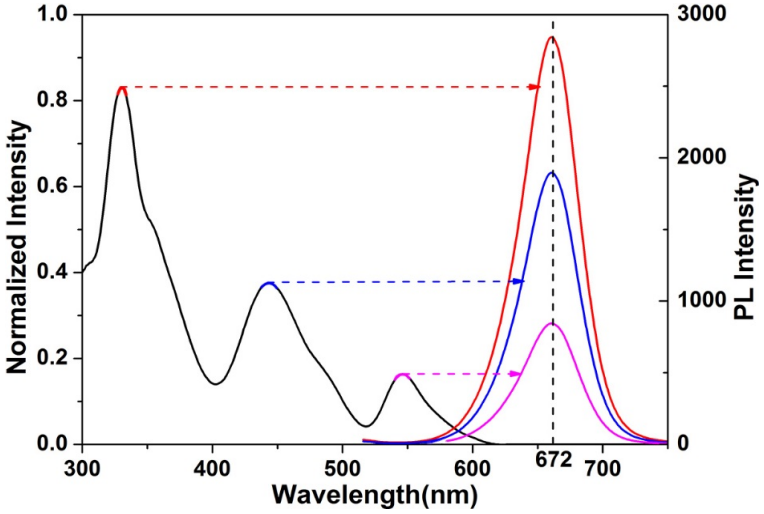


**Fig. S9.** Photoluminescence properties of $Pt_1Ag_{28}(S\text{-}Adm)_{18}(PPh_3)_4$. Excitation spectrum (left) and emission spectra (right) at different excitation wavelengths, as indicated by the arrows.

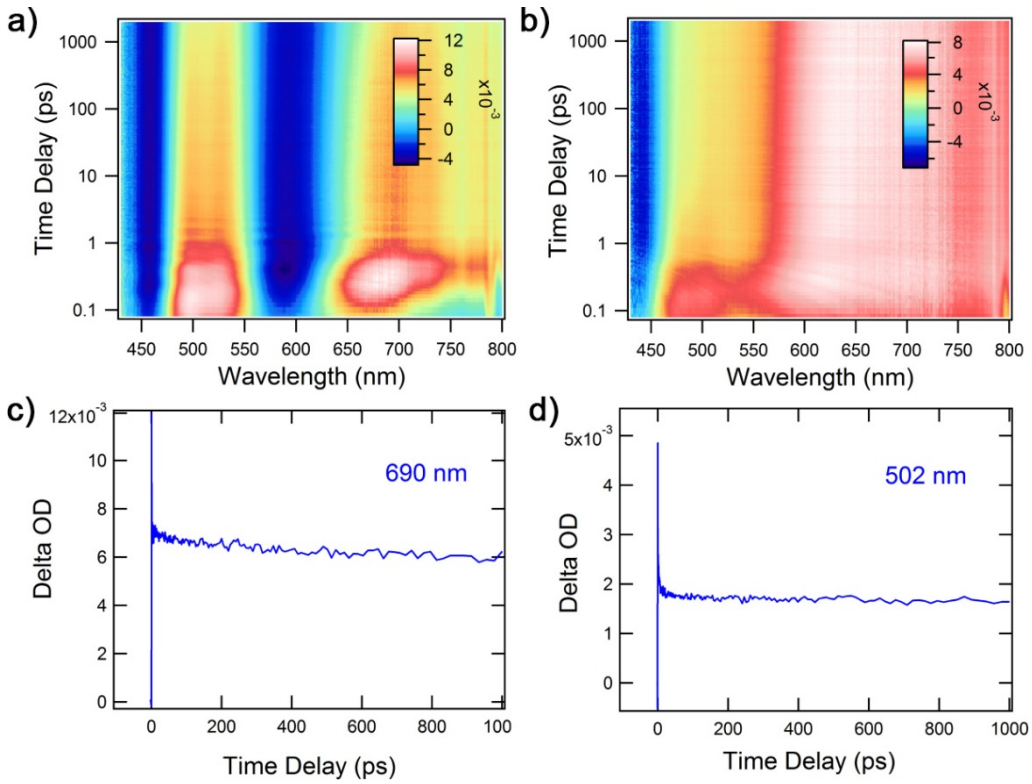


**Fig. S10.** Femtosecond transient absorption data map at all time delays (0.1 ps to 3 ns) and probe wavelengths for a) $Pt_1Ag_{24}$ and b) $Pt_1Ag_{28}$ nanoclusters with excitation of 360 nm. c, d) Kinetic traces at selected wavelengths between -1 ps and 1 ns for c) $Pt_1Ag_{24}$ and d) $Pt_1Ag_{28}$.

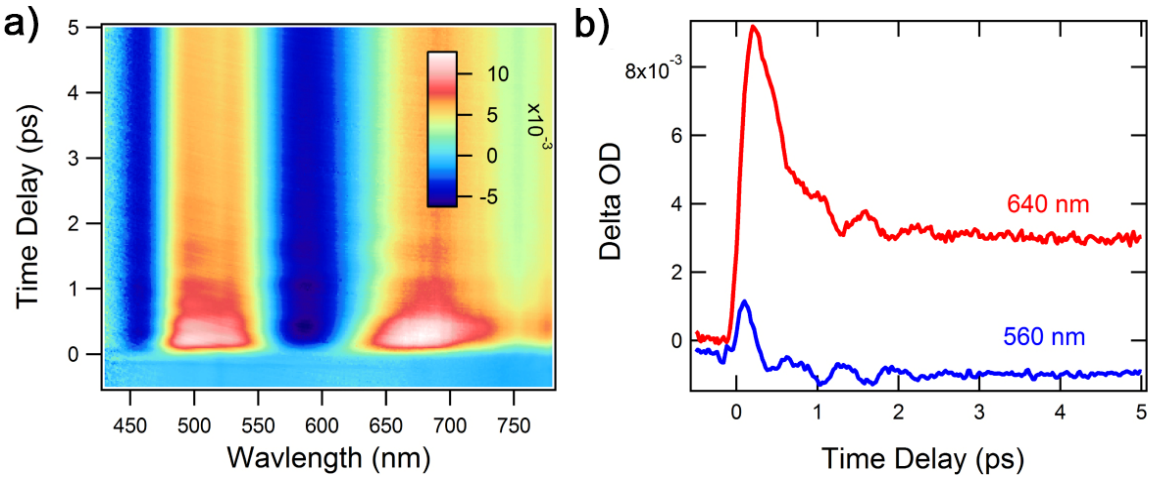


**Fig. S11.** a) Femtosecond transient absorption data map of $Pt_1Ag_{24}$ at early time delays (-0.5 ps to 5 ps). b) Coherent oscillations observed in kinetic traces at selected wavelengths.

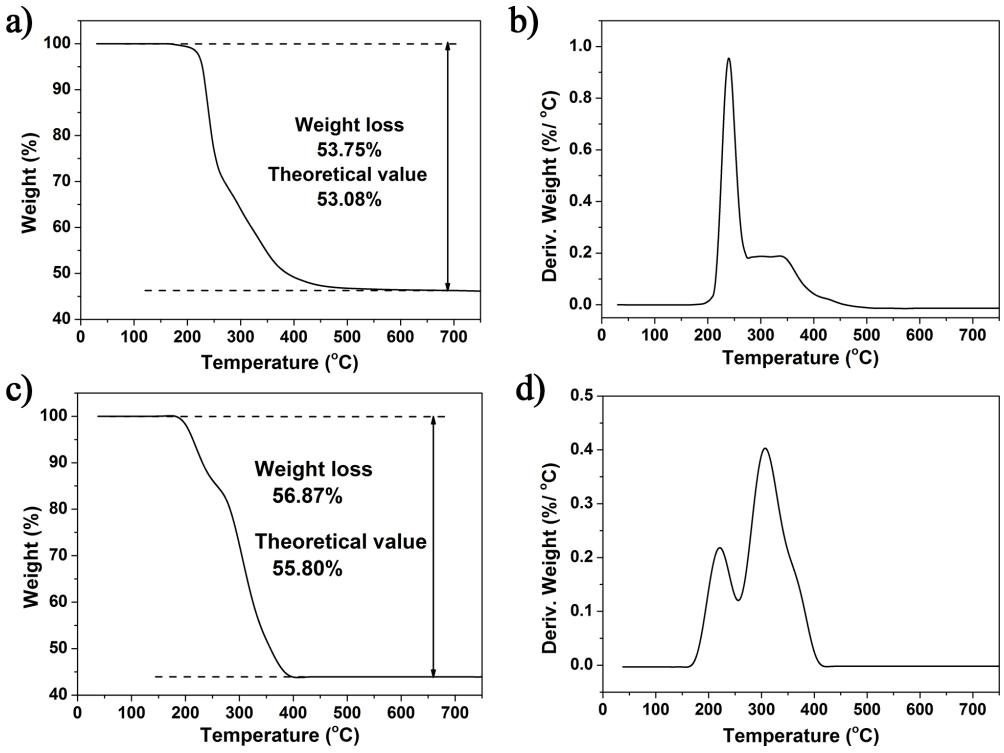


**Fig. S12.** a) TGA curve and b) the derivative of $Pt_1Ag_{24}$; c) TGA curve and d) the derivative of $Pt_1Ag_{28}$.

**Table S1.** The atom ratio of Pt and Ag in $Pt_1Ag_{28}(S\text{-}Adm)_{18}(PPh_3)_4$ nanocluster calculated from inductively coupled plasma (ICP) and X-ray photoelectric spectroscopy (XPS) measurements.

| | Pt atom | Ag atom |
|---|---|---|
| ICP Experiment ratio of $Pt_1Ag_{28}(S\text{-}Adm)_{18}(PPh_3)_4$ | 3.9% | 96.1% |
| XPS Experiment ratio of $Pt_1Ag_{28}(S\text{-}Adm)_{18}(PPh_3)_4$ | 3.5% | 96.5% |
| Theoretical ratio of $Pt_1Ag_{28}(S\text{-}Adm)_{18}(PPh_3)_4$ | 1/29(3.45%) | 28/29(96.55%) |

**Table S2**. Structural analysis of $Ag_{29}$, $Au_1Ag_{28}$ and $Pt_1Ag_{28}$ nanoclusters.

| | M(center)-Ag lengths in the kernel (Å) | Ag-S lengths on the kernel-shell (Å) | Ag-Ag lengths on the kernel-shell (Å) | P-Ag-S angles on the same motifs ($^o$) |
|---|---|---|---|---|
| $Ag_{29}$ | 2.755-2.772 | 2.433-2.474 | 3.077-3.158 | 104.12-109.19 |
| Averages | 2.765 | 2.459 | 3.111 | 106.91 |
| $Au_1Ag_{28}$ | 2.745-2.775 | 2.425-2.472 | 3.123-3.161 | 104.50-108.63 |
| Averages | 2.761 | 2.444 | 3.141 | 105.94 |
| $Pt_1Ag_{28}$ | 2.768-2.797 | 2.438-2.498 | 2.934-3.157 | 119.28-131.46 |
| Averages | 2.783 | 2.472 | 3.104 | 126.80 |

**Table S3.** Excited state lifetimes of silver and doped silver nanoclusters.

| Sample | Excited State Lifetimes |
|---|---|
| $Ag_{25}$[1] | 1.1 μs |
| $Pt_1Ag_{24}$ | 1.9 μs |
| $Ag_{29}$[2] | 350 ns |
| $Pt_1Ag_{28}$ | 300 ns, 2.9 μs |

**Table S4**: Crystal data and structure refinement for the $Pt_1Ag_{28}(S\text{-}Adm)_{18}(PPh_3)_4$ nanocluster.

| | | |
|---|---|---|
| Compound reference | $Pt_1Ag_{28}(S\text{-}Adm)_{18}(PPh_3)_4$ | |
| Empirical formula | C252H330Ag28PtP4S18 | |
| Formula weight | 7275.55 | |
| Temperature | 143 K | |
| Wavelength | 1.54178 Å | |
| Crystal system | Monoclinic | |
| Space group | C 2/c | |
| Unit cell dimensions | A=50.8135 (18) Å | $\alpha$=90° |
| | B=29.3497(8)Å | β=110.274(4)° |
| | C=49.1614(16)Å | γ=90° |
| Volume | 68775(4) $Å^3$ | |
| Z | 8 | |
| Density (calculated) | 1.405 Mg $m^{-3}$ | |
| Absorption coefficient | 14.666 $mm^{-1}$ | |
| F(000) | 28272 | |
| Crystal size | 0.05 × 0.03 × 0.02 $mm^3$ | |
| Theta range for data collection | 3.01 to 55.95° | |
| Index ranges | -63<=h<=59, -34<=k<=36, -57<=l<=61 | |
| Reflections collected | 239535 | |
| Independent reflections | 67855 | |
| Absorption correction | Multi scan | |
| Refinement method | SHELXL-2014/7 (Sheldrick 2014/7) | |
| Data / restraints / parameters | 67855 / 8 / 2728 | |
| Goodness-of-fit on F2 | 1.048 | |
| Final R indices [I>2sigma(I)] | R1=0.0333, wR2=0.0845 | |
| R indices (all data) | R1=0.0432, wR2=0.0867 | |

**References.**


[1] Bootharaju, M. S., Joshi, C. P., Parida, M. R., Mohammed, O. F. & Bakr, O. M. Templated atom-precise galvanic synthesis and structure elucidation of a $[Ag_{24}Au(SR)_{18}]$ nanocluster. *Angew. Chem. Int. Ed.* **55**, 922-926 (2016).

[2] Soldan, G., Aljuhani, M. A., Bootharaju, M. S., AbdulHalim, L. G., Parida, M. R., Emwas, A. –H., Mohammed, O. F. & Bakr, O. M. Gold doping of silver nanoclusters: a 26-fold enhancement in the luminescence quantum yield. Angew. Chem. Int. Ed. 55, 5749-5753 (2016).

[3] AbdulHalim, L. G., Bootharaju, M. S., Tang, Q., Gobbo, S. D., AbdulHalim, R. G., Eddaoudi, M., Jiang, D. –en. & Bakr, O. M. $Ag_{29}(BDT)_{12}(TPP)_4$: a tetravalent nanocluster. J. Am. Chem. Soc. 137, 11970-11975 (2015).